Contents lists available at ScienceDirect

Environmental Impact Assessment Review

journal homepage: www.elsevier.com/locate/eiar

Lifecycle emissions of hydrogen supply chains in China: A spatially resolved assessment

Fangjie Liu [a], Muhammad Shafique [b,*], Xiaowei Luo [a,*]

[a] Department of Architecture and Civil Engineering, City University of Hong Kong, Hong Kong, China
[b] Department of Civil and Environmental Engineering, Brunel University of London, Uxbridge, Middlesex, UK

ARTICLE INFO

Keywords:
Hydrogen mobility
Hydrogen delivery systems
Lifecycle assessment
Transport routes
Spatial heterogeneity
Regional energy systems
Ultra-high voltage transmission
Carbon emissions
Energy carriers

ABSTRACT

Current hydrogen delivery assessments exhibit incomplete supply chain coverage, insufficient carrier diversity, and oversimplified spatial analysis relying on hypothetical distances. This study addresses these limitations through comprehensive life cycle assessment across China's four major transport routes for 2030–2060, evaluating 12 delivery systems comprising four transportation modes (pipeline, truck, ship, ultra-high-voltage transmission) and six hydrogen carriers across 25 sub-routes with actual geographic constraints and provincial energy profiles. Results reveal that spatial heterogeneity in regional energy systems rather than transport distance constitutes the primary determinant of delivery emissions. For the same delivery mode, emissions varied markedly across provinces because of differences in electricity carbon intensity, from 0.64 kg CO_2eq/kg H_2eq for Pipeline-CGH_2 on Yunnan–Guizhou to 1.98 kg CO_2eq/kg H_2eq on Inner Mongolia–Shanxi in 2030. Non-optimal mode selection further caused large emission penalties, especially in high-carbon routes and in later years. UHV-electricity transmission achieves the lowest emissions across 88% of sub-routes (0.03–0.31 kg CO_2eq/kg H_2eq by 2060), while ship-based transport demonstrates competitive performance in only one of three waterway-accessible routes, with this advantage reversing by 2060 due to accelerating grid decarbonization. Lifecycle stage decomposition indicates delivery-stage emissions dominate truck-based systems (>60%), while post-delivery processing dominates carrier-based modes. These findings demonstrate that hydrogen infrastructure planning requires regionally-differentiated strategies: priority UHV deployment for northwestern-to-eastern routes where emission disparities between optimal and suboptimal modes are most substantial, flexible multi-modal approaches for southwestern routes, and selective waterway infrastructure investment. This spatially-explicit framework provides evidence-based guidance demonstrating that regional energy profiles fundamentally shape delivery system performance beyond conventional distance-based optimization.

1. Introduction

Climate change and its associated impacts have intensified in recent years, underscoring the urgency of global decarbonization efforts. In 2024, China recorded its warmest year on record, with the national average temperature rising approximately 1.03 °C compared to 2023, accompanied by severe and frequent extreme weather events (Zhao, 2025). Similarly, during January 2025, wildfires in California resulted in 57 billion USD in losses and extensive vegetation combustion, releasing substantial amounts of carbon dioxide and severely degrading air quality (Mittal, 2025). Research by Wang et al. (2025a) reveals that climate change significantly intensifies China's low-carbon power transition challenges, with projected system cost increases of 20% by 2050. These developments emphasize the critical need for coordinated international efforts in carbon emission reduction and accelerating the transition toward a net-zero carbon society.

Abbreviations: AI, Artificial intelligence; B20, 20% biodiesel blend; CGH_2, Compressed gas hydrogen; CI, Carbon intensity; EI, Environmental impact; ETC, Energy Transitions Commission; GA, Green ammonia; GH, Green hydrogen; GWP, Global warming potential; H_0DBT/DBT, Dibenzyltoluene; H_{12}NEC, Perhydro-N-ethylcarbazole; H_{18}DBT/PDBT, Perhydro-dibenzyltoluene; ISO, International Organization for Standardization; LCA, Life cycle assessment; LCOT, Levelized cost of transportation; LH_2, Liquid hydrogen; LHSEP, Liquid hydrogen superconducting energy pipeline; LHV, Low heating value; LOHC, Liquid organic hydrogen carrier; MCH, methyl cyclohexane; MeOH, Methanol; NEC, N-ethylcarbazole; NH_3, Ammonia; R&D, Research and development; RMI, Rocky Mountain Institute; TOL, Toluene; UHV, Ultra-high-voltage.

* Corresponding authors.
E-mail addresses: muhammad.shafique@brunel.ac.uk (M. Shafique), xiaowluo@cityu.edu.hk (X. Luo).

https://doi.org/10.1016/j.eiar.2026.108435
Received 19 June 2025; Received in revised form 19 December 2025; Accepted 14 March 2026

Achieving carbon neutrality requires integrating technological innovation with institutional reforms across multiple domains. Key pathways include energy efficiency optimization through smart grids and AI-driven building management systems (Alaba et al., 2024; Baz et al., 2024), large-scale renewable energy adoption via wind-solar-hydrogen-storage integration (Boretti, 2025; Sun et al., 2025), carbon sink enhancement through biochar sequestration and algae-based carbon capture (Deng et al., 2025; Sinyoung et al., 2025), green finance mechanisms incorporating climate risk governance (Yang et al., 2024), and systemic industrial transitions demonstrated by zero-carbon park designs (Yin et al., 2024). Empirical evidence supports these approaches: Hamburg's district energy systems have achieved 30% energy consumption reduction in public buildings (EIT, 2025), while China's Ordos Industrial Park is pioneering renewable-powered hydrogen-based decarbonization (China Daily, 2025). Research in China demonstrates that coordinated renewable energy policy combinations, particularly those integrating market mechanisms with mandatory consumption policies, have proven significantly more effective than individual policies in accelerating power sector decarbonization (Wang et al., 2025b).

The widespread adoption of clean hydrogen energy represents a critical component in global decarbonization strategies (Rumsa et al., 2025; Shao et al., 2024; Zhang et al., 2024). However, systemic impediments limit its commercial scalability. Significant challenges persist in establishing cross-regional hydrogen supply chains due to infrastructure inadequacies for long-distance transportation of gaseous or cryogenic hydrogen (Boretti and Pollet, 2024). High-pressure pipeline systems face material degradation risks and fugitive emission vulnerabilities (Nanninga et al., 2012). While truck-based logistics of liquid hydrogen require energy-intensive cryogenic containment technologies that increase operational expenditures by 11–33% relative to liquid organic hydrogen carrier (LOHC) supply chains (Niermann et al., 2021). Lifecycle emissions assessment presents another challenge, requiring rigorous quantification of carbon intensity across production, storage, and distribution stages. Renewable-powered electrolytic hydrogen demonstrates a carbon footprint below 1 kg CO_2/kg H_2, while conventionally steam-reformed hydrogen exceeds 10 kg CO_2/kg H_2 (Savickas, 2022). Noh et al. (2023) showed that the electricity source strongly affects lifecycle emissions in offshore hydrogen supply chains: when national grid electricity and offshore wind power were used together, GWP ranged from 1.15 to 10.11 kg CO_2 eq, compared with 1.15 to 2.05 kg CO_2 eq when only offshore wind power was used. Their results also indicate that energy-intensive downstream steps, such as dehydrogenation and ammonia cracking, remain important contributors to total environmental load. Khatiwada et al. (2022) reported 2020 production costs of 1.33 €/kg H_2 for grey hydrogen and 1.68 €/kg H_2 for blue hydrogen, compared with 3.54–4.65 €/kg H_2 for green hydrogen produced by PEM electrolysis using solar or grid electricity.

These challenges demonstrate the complex interplay between technological, economic, and regulatory dimensions in establishing sustainable hydrogen supply chains. A comprehensive review of recent advancements and research is essential for addressing these barriers and accelerating the global transition to a hydrogen-based, low-carbon future.

2. Literature review

2.1. Current state of hydrogen and hydrogen carrier storage/delivery technologies

Current hydrogen or hydrogen carrier storage methods can be broadly categorized into physical and chemical approaches (Liu et al., 2025a). Physical storage methods preserve the chemical characteristics of hydrogen and include compressed hydrogen and liquid hydrogen. Chemical storage methods involve hydrogen carriers that require chemical reactions for hydrogen release, including inorganic chemical hydrogen storage carriers such as ammonia (NH_3) and methanol (MeOH) (El Hassani et al., 2024), as well as organic carriers such as dibenzyltoluene (H_0DBT)/perhydro-dibenzyltoluene (H_{18}DBT) and N-ethylcarbazole (NEC)/perhydro-N-ethylcarbazole (H_{12}NEC), which are referred to as LOHCs (Sage et al., 2024). Hydrogen and its carriers are stored in specially designed tanks, with the specific type determined by the physicochemical properties of the medium (Alkhaledi et al., 2022; Drube et al., 2024). Compressed hydrogen is stored in high-pressure tanks, liquid hydrogen requires cryogenic insulated tanks (Winnefeld et al., 2018), while ammonia and LOHCs can be stored in conventional liquid tanks (Li et al., 2024a).

Recent studies have explored advances in tank technologies and carrier selection. Drube et al. (2024) found that prismatic tank designs improved liquid hydrogen storage capacity by 26% for hydrogen powered vessels. Alkhaledi et al. (2022) proposed the JAMILA tanker design featuring large LH_2 tanks and hydrogen-fuelled gas turbine for efficient, sustainable shipping. Gambini et al. (2024) evaluated LOHC-based hydrogen storage for maritime applications, finding that while LOHC systems provide adequate dynamic performance, ammonia emerges as a more efficient option for large-scale maritime applications.

Hydrogen and hydrogen carrier transportation encompasses multiple modalities, including tube trailers, pipelines (Gillette and Kolpa, 2008), maritime tankers (Godinho et al., 2023), rail transport, and ultra-high-voltage (UHV) electricity transmission. The selection of transportation methods is closely linked to storage requirements, as liquid hydrogen's cryogenic storage requirements preclude pipeline transportation. Liu et al. (2025a) identify that generation scenarios govern storage-delivery configurations through energy distribution patterns, storage stability thresholds, and regional accessibility constraints. Reddi et al. (2018) analyzed hydrogen delivery via tube trailers, finding that advanced composite trailers can transport larger payloads and reduce delivery costs by up to 16% for long-distance transport. Xu et al. (2024) analyzed hydrogen delivery for railway refueling in the UK, finding that while compressed gas hydrogen (CGH_2) road delivery is sufficient initially, growing hydrogen demand will require LH_2 and rail transport for long-distance supply.

2.2. Advances in life cycle assessment methodology for hydrogen carrier delivery systems

Life cycle assessment (LCA) serves as a tool for evaluating cradle-to-grave environmental footprints of a product (Shafique et al., 2022) such as hydrogen delivery systems. The environmental and economic effects of hydrogen delivery systems vary depending on geographical location, energy structure, transportation volume, and distance. Despite methodological advancements, challenges persist due to inconsistencies in system boundaries and lack of transparency in methodologies, which limit comparability and harmonization across studies.

Several studies have analyzed LOHC-based hydrogen delivery systems. Godinho et al. (2023) analyzed LOHC-based hydrogen delivery via maritime shipping within Europe, reporting logistics costs between 0.28 and 0.37 EUR/kg-H_2 and associated CO_2 emissions of 0.46–2.95 kg CO_2/GJ (LHV) from 2030 to 2050, depending on the type of LOHC. Rey et al. (2024) conducted a comprehensive LCA of platinum-based catalysts used in LOHC systems, identifying dehydrogenation as the most impactful step in hydrogen supply chains based on the LOHC H_0-BT/H_{12}-BT system, contributing 54.35% of the global warming potential (GWP). Their sensitivity analysis demonstrated that substituting primary platinum with recycled platinum in catalyst synthesis can substantially reduce environmental impacts across multiple categories, with endpoint impact reductions ranging from 41.41% to 96.27% depending on the catalyst type (Rey et al., 2024). Ship transport was found to account for 12.48% of total GWP in the hydrogen supply chain based on LOHC systems (Rey et al., 2024).

Cho et al. (2024) found dehydrogenation to account for 46.4% of GWP, followed by transport at 15.6%. Renewable toluene showed lower production emissions compared to DBT, and the use of wind electricity and biodiesel (B20) reduced impacts by 51%. Godinho et al. (2024) showed that LOHC-based systems in China could reduce delivery costs by 2–4% compared to gaseous or liquefied hydrogen while reducing CO_2 emissions by 52–67% by 2060.

Beyond LOHCs, green ammonia (GA) has been studied as a hydrogen carrier for international supply chains. Kim et al. (2024) identified GA as having advantages over green hydrogen (GH) due to its storage and transport properties, with a case study on nine trading routes demonstrating its economic efficiency. Ahn et al. (2024) examined the environmental impacts of hydrogenation the toluene-methylcyclohexane (TOL-MCH) LOHC system, noting 13% higher fossil resource scarcity and 746% higher water use in hydrogenation compared to other processes. Notably, their analysis demonstrated that replacing natural gas with renewable or nuclear energy sources for process heat could achieve net-negative GWP values due to avoided grid electricity emissions, resulting in a 111% reduction compared to the natural gas baseline (Ahn et al., 2024).

Pipeline transmission systems also contribute to hydrogen delivery, providing scalable and cost-effective solutions for large-scale transport. Yu et al. (2024) developed a techno-economic model for hydrogen pipeline networks, reporting the levelized cost of transportation (LCOT) values ranging from 0.13 to 1.81 USD/kg depending on design pressure, annual transmission volume, and transportation distance. Sayer et al. (2024) found pipeline transport to be less expensive than shipping for hydrogen delivery from North Africa to Europe, noting the importance of renewable energy expansion and the repurposing of gas pipelines to reduce costs and emissions. Balaji and You (2024) evaluated offshore wind-based green hydrogen delivery systems, reporting delivered costs ranging from 2.50 to 7.00 USD/kg H_2 with lifecycle emissions below 4 kg CO_2eq/kg H_2, finding compressed hydrogen pipelines more cost-effective and environmentally favorable than liquefied hydrogen shipping.

2.3. Methodological limitations in current hydrogen supply chain assessments

Current hydrogen supply chain assessments exhibit critical methodological limitations that prevent accurate comparative analysis and system optimization. These limitations extend beyond scope coverage to fundamental issues of comparability, spatial representation, and temporal dynamics.

The lack of standardized comparative frameworks creates substantial inconsistencies across studies. As Gonçalves Dias Ponzi et al. (2024) demonstrated, this harmonization gap extends to basic definitions, with "low-carbon hydrogen" thresholds varying from 4.4 to 14.5 kg CO_2eq/kg H_2 across different certification schemes. Most assessments oversimplify spatial heterogeneity by using averaged conditions that mask critical regional variations. Chen et al. (2024) exemplified this limitation by analyzing hydrogen pathways using national average emission factors, overlooking substantial provincial differences in energy structures. This oversimplification is particularly problematic for energy-intensive processes like compression and liquefaction, where local electricity profiles fundamentally alter system performance.

Current studies also fail to capture the dynamic evolution of hydrogen supply chains, predominantly employing static scenarios despite projected massive scaling through 2050. While Makepeace et al. (2024) projected that 85% of future hydrogen demand will require interregional transport, their analysis used fixed parameters without considering temporal changes in technology performance or energy systems. Shen et al. (2024) identified evolving trade-offs in green hydrogen deployment, including carbon reduction benefits of up to 91% accompanied by increased resource demands, yet most assessments fail to capture how these dynamics shift comparative advantages over time.

Fragmented evaluation approaches and lifecycle stage aggregation further limit comprehensive system understanding. Studies typically examine delivery options in isolation, as illustrated by Qin et al. (2024) focusing exclusively on liquid hydrogen superconducting pipelines. While demonstrating innovative solutions, such singular focus prevents identification of modal transition points where alternative methods become preferable based on distance, volume, or regional characteristics. Additionally, lifecycle stage aggregation in reporting obscures optimization opportunities within the supply chain. de Kleijne et al. (2024) assumed uniform clean electricity for pre-delivery processes, yet actual implementation involves varying regional grids that fundamentally alter stage-specific contributions.

2.4. Innovation of the research

This study introduces innovations in the analysis of hydrogen delivery systems, and it addresses existing gaps in the literature regarding hydrogen storage and transportation processes. The main contributions are as follows:

First, this study provides a future-oriented complete supply chain assessment. While existing studies analyze complete hydrogen supply chains, they primarily focus on current technology scenarios. Based on the understanding that future decarbonization efforts will rely on green hydrogen production using clean energy sources, this study analyzes complete supply chain stages (pre-delivery, delivery, post-delivery) under future green energy scenarios. This approach provides insights for supply mode selection and infrastructure planning in a decarbonized energy system.

Second, this study achieves complete carrier and mode coverage. The study analyzes 12 hydrogen delivery systems, composed of four transportation modes (truck, pipeline, ship, UHV-electricity) and six hydrogen or hydrogen carrier options (CGH_2, LH_2, MeOH, DBT, NH_3). Existing studies focus on limited comparisons such as LOHC versus compressed/liquid hydrogen or include selected inorganic carriers like NH_3. In contrast, this study covers the complete spectrum of both organic carriers and inorganic carriers alongside traditional hydrogen forms, enabling comparative evaluation within a unified assessment framework.

Third, this study implements real-world spatiotemporal analysis. Most existing studies either rely on abstract assumptions (e.g., hypothetical 1000 km, 2000 km transport distances) or consider simplified real-world scenarios with few actual distances. This analysis integrates actual geographic constraints, real transport distances, and projected delivery volumes across China's four major transport routes comprising 25 sub-routes. The approach accounts for spatiotemporal variability of energy structures across different regions and for temporal changes in hydrogen transportation demand from 2030 to 2060, providing contextually relevant results applicable to real-world implementation scenarios.

By integrating these elements, the study provides a comprehensive evaluation of hydrogen delivery systems, contributing insights to the development of hydrogen supply chains in the context of achieving net-zero emissions.

3. Methodology

This study adopts a comprehensive life cycle assessment (LCA) approach following the standardized framework established by ISO 14040 (ISO, 2006a) and ISO 14044 (ISO, 2006b) standards, consisting of four phases: goal and scope definition, inventory analysis, impact assessment, and interpretation. This methodological approach aligns with UNEP guidelines for LCA harmonization (UNEP, 2009), ensuring consistency with internationally recognized environmental assessment frameworks and supporting comparative analysis across diverse hydrogen delivery scenarios.

The functional unit is 1 kg of hydrogen equivalent (per kg H_2eq) delivered to the demand location, consistent with established practices in hydrogen transportation LCA research. To ensure fair comparison across all pathways, the delivered hydrogen is assumed to be at a standardized end-state suitable for hydrogen refueling station storage: a pressure of 30 bar and a purity level of ≥99.97%, consistent with ISO 14687 (ISO, 2025) requirements for fuel cell vehicle applications. For pathways utilizing chemical carriers (NH_3, MeOH, LOHC), all conversion and purification processes necessary to achieve this end-state are included within the system boundary. This functional unit choice aligns with the consensus observed across major hydrogen delivery studies, where kg serves as the standard transport quantity assessment criterion and km as the transport distance criterion (Liu et al., 2025a). Professional organizations and research institutions consistently employ per kg H_2 and per km as primary functional units in hydrogen logistics assessments (BloombergNEF, 2020; ETC, 2021), reflecting their appropriateness for comparative analysis across diverse delivery scenarios. The term 'hydrogen equivalent' is used to account for the fact that hydrogen may be transported in various chemical forms (LH_2, NH_3, MeOH, or LOHC), and the functional unit represents the hydrogen content that can ultimately be recovered and delivered to end users at the specified reference conditions. The selection of kg H_2eq enables fair comparison across different hydrogen carriers and delivery modes without assuming specific production pathways, thereby supporting comprehensive environmental assessment within the defined system boundary. This unit supports two analytical perspectives. When assessing the environmental impacts of an entire hydrogen delivery network, this unit allows for comprehensive evaluation of the cumulative emissions or impacts without normalizing by transportation distance, thereby providing an understanding of the overall environmental burden of the full delivery pathway. The "per kg H_2-eq" unit itself does not account for distance. However, Section 4.3 presents scatter plots to visualize and analyze the environmental impacts per unit distance. These plots offer insights into how different delivery modes perform environmentally across various transport distances. They complement the overall impact assessment provided by the functional unit and enable detailed comparison of how different delivery methods perform.

Before conducting the inventory analysis, the system boundary must be established to define the scope of processes included in the assessment. The system boundary determines which stages of the hydrogen delivery system are analyzed. Following ISO 14040 principles for system boundary delineation, these include pre-delivery (e.g., hydrogenation for liquid organic hydrogen carriers), delivery, and post-delivery (e.g., dehydrogenation). After this, the inventory list is developed to identify and quantify the inputs and outputs associated with each stage within the system boundary. The inventory analysis adheres to ISO 14044 (ISO, 2006b) data quality requirements, incorporating primary data from established databases (Argonne National Laboratory, 2022) and peer-reviewed literature sources to ensure methodological transparency and reproducibility as emphasized in UNEP frameworks (UNEP, 2009). Data collection follows systematic approaches with clear documentation of sources, temporal representativeness, and geographical coverage. Regional electricity grid profiles ensure spatial representativeness, while temporal coverage spans 2030–2060 to capture technology evolution dynamics. The impact assessment follows the ISO 14044 framework (ISO, 2006b) for life cycle impact assessment, focusing on climate change impact category through greenhouse gas emissions quantification. The selection of GHG-100 parameter from the GREET model represents the environmental greenhouse gas impact over a 100-year timeframe, consistent with IPCC characterization factors widely accepted in LCA practice (Masson-Delmotte et al., 2021). The subsequent sections of the methodology provide detailed explanations of the system boundary definition, data sources, and data processing methods used for inventory analysis.

3.1. System boundary definition

The analysis was conducted using the GREET software for core LCA calculations. Secondary data processing, analysis, and visualization were performed in Python. Building on the insights from Liu et al. (2025a), this research focuses on evaluating hydrogen delivery systems. The evaluation covers the entire supply chain from pre-delivery preparation to post-delivery conditioning.

Fig. 1 illustrates the research framework for analyzing hydrogen transportation systems. The framework integrates dataset inputs (energy consumption parameters, regional grid data from GREET and IEA, and carrier-specific efficiencies) and system boundaries spanning pre-delivery (hydrogen compression, carrier synthesis), delivery (transport via pipeline, truck, ship, or UHV using physical, chemical, or energy-mediated carriers), and post-delivery stages (decompression, dehydrogenation). The framework highlights the interdependencies between spatial factors, transportation modes (CGH_2, NH_3, DBT, etc.), and process efficiencies. This allows comparison of emissions and energy use across supply chains (Liu et al., 2025a).

The system boundary begins with produced hydrogen or its carrier (CGH_2, LH_2, ammonia (NH_3), or LOHCs such as DBT) and ends with hydrogen delivered as compressed hydrogen for transportation applications. The analysis includes pre-delivery processes (compression, hydrogenation, or synthesis), delivery via pipelines, trucks, ships, or UHV transmission, and post-delivery steps (decompression, dehydrogenation, or carrier cracking).

The selection of transportation modes and hydrogen carriers was based on commercial viability projections from INTEGRAL institute reports and the China Hydrogen Alliance white papers on hydrogen and fuel cell industry development (China Hydrogen Alliance, 2019; INTEGRAL, 2021). These sources identify three primary carrier categories for near-term through long-term commercial deployment: gaseous hydrogen, liquid hydrogen, and alternative hydrogen carriers. Four transportation modes (pipeline, truck, ship, UHV) and six hydrogen carriers (CGH_2, LH_2, NH_3, methanol (MeOH), DBT, and electricity) were analyzed based on this framework. Near-term implementation is expected to focus on gaseous and liquid hydrogen transport via pipelines and trucks, while long-term scenarios include ship-based liquid hydrogen transport and alternative carriers including LOHCs. These carriers were classified into physical carriers (CGH_2, LH_2), chemical carriers (organic: DBT; inorganic: NH_3, MeOH), and energy-mediated carriers (electricity). While data availability constraints prevented inclusion of all potential carriers such as solid carriers, the study ensures representation of each carrier category through at least one representative option. For LOHC selection, H_0DBT/H_{18}DBT was chosen as the representative due to data accessibility, while other notable LOHC options including MCH/TOL and H_{12}-NEC/NEC pairs were excluded due to limited data availability despite their recognized potential in current research (Sage et al., 2024). Data inputs included energy consumption and emission factors from the GREET database, region-specific electricity grid profiles (China Electricity Council, 2022; Ren et al., 2023), and carrier-specific parameters (hydrogenation efficiency, liquefaction energy) from peer-reviewed literature or reports (Arrigoni et al., 2024; Li et al., 2024b; Liu et al., 2025b; Liu et al., 2024). Emissions and energy use were normalized per kilogram of delivered hydrogen, accounting for spatial variations in energy structure, delivery distances, and reaction processes.

A fuller explanation of the system boundary requires integration with the data inputs. Therefore, Section 3.2, which describes data inputs and model configurations, will provide a more comprehensive presentation of the methodological logic and aspects of this study.

3.2. Data collection and simulation settings

This section introduces the data inputs and model configurations. Building upon the system boundaries and framework outlined in Section 3.1, the data inputs are categorized into three components: (1) the power grid and energy mix of the origin and destination provinces for each transportation route; (2) the delivery distance for each route, which varies depending on the mode of transportation; and (3) the material inventories for the pre- and post-delivery stages of each

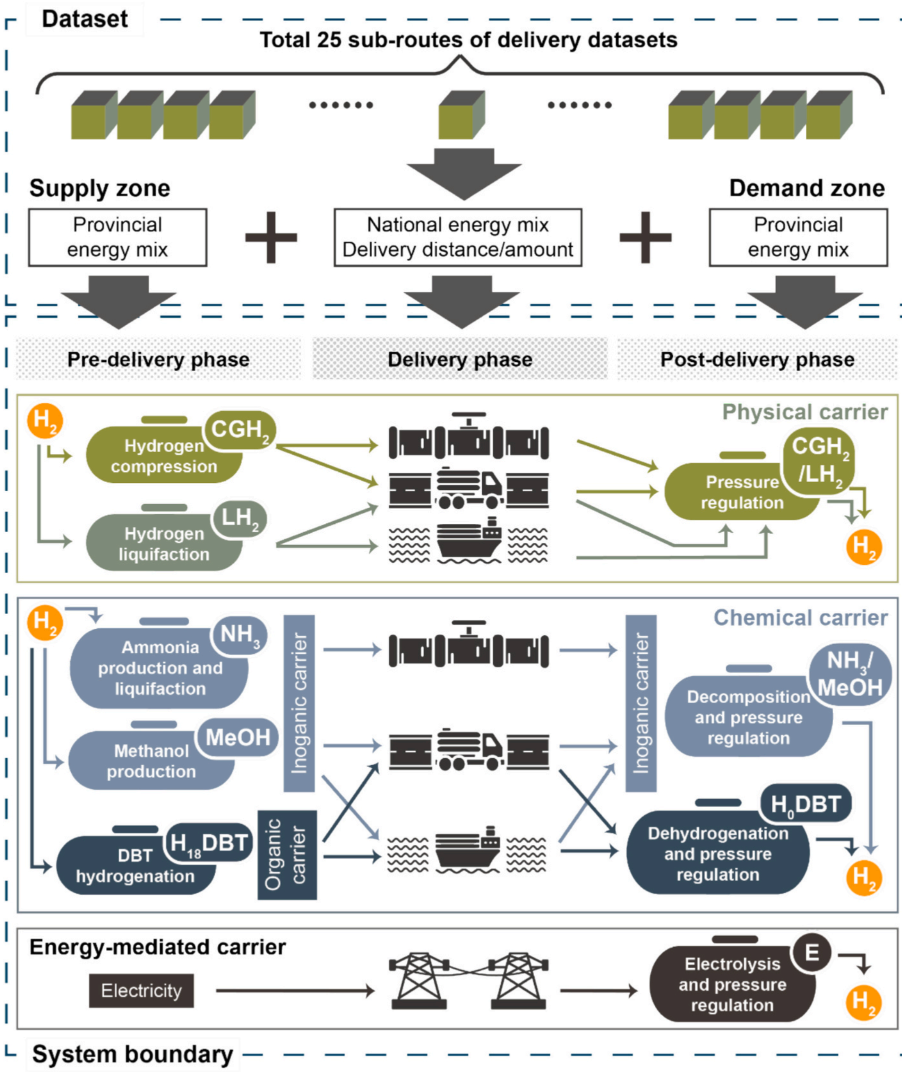

Fig. 1. System boundary and framework (Abbreviation explanation: CGH_2-compressed gas hydrogen; LH_2-liquid hydrogen; NH_3- ammonia; MeOH-methanol; DBT-Dibenzyltoluene).

delivery mode. The data inputs and configurations are summarized in Table 1, while other inputs and settings are based on the default parameters of the GREET model and can be referenced in the following explanations and Supplementary Tables 1–2. For the LOHC pathway utilizing DBT as the carrier, the dehydrogenation of DBT-H_{18} is an endothermic process requiring substantial heat input. Following the approach established by Arrigoni et al. (2024), we assume that this heat is provided by combusting a portion of the hydrogenated LOHC itself. Specifically, for every 16.3 kg of DBT-H18 processed to release 1 kg of hydrogen product, an additional 10 kg of DBT-H18 is combusted to supply the required process heat. This assumption is reflected in the life-cycle inventory presented in Supplementary Table 9. To ensure transparency and enable replication of our analytical approach, comprehensive methodological details are provided in the supplementary materials. Supplementary Tables 3–9 contain detailed assumptions and parameters beyond GREET's default settings, while comprehensive emission factors are presented in detailed tables within the appendix of Liu et al. (2024). The information provided in the manuscript and supplementary materials contains sufficient detail for independent researchers to configure equivalent GREET scenarios and verify our analytical framework. This documentation approach balances methodological transparency with practical research considerations while providing the complete foundation necessary for independent replication and validation of our results.

Table 1
Data resources.

Variable name	Resource information	Ref.
Electricity carbon intensity	Provincial electricity grid mix	(Liu et al., 2025b)
Hydrogen delivery landscape (4 main routes)	Long term outlook on hydrogen storage and transportation landscape and technology evolution in China	RMI (Li et al., 2024b)
Hydrogen and hydrogen carrier reaction inventory	Environmental life cycle assessment (LCA) comparison of hydrogen delivery options within Europe	(Arrigoni et al., 2024)

Several details require explanation and clarification. Regarding data inputs, the report by RMI (Li et al., 2024b) identifies four hydrogen supply and demand routes in China for the midium- to long-term. These include: (1) from Inner Mongolia to Heilongjiang, Jilin, Liaoning, Beijing, Tianjin, Hebei, and Shanxi; (2) from Xinjiang, Gansu, and Qinghai to Ningxia, Shaanxi, Henan, Shandong, and Jiangsu; (3) from Tibet and Sichuan to Chongqing, Hubei, Anhui, Jiangxi, Zhejiang, Fujian, and Shanghai; and (4) from Yunnan to Guizhou, Hubei, Guangxi, Guangdong, and Hainan.

The RMI report establishes fixed aggregate supply-demand quantities for each major route derived from detailed regional production capacity assessments and long-term consumption forecasting. Based on these predetermined supply-demand relationships provided in the RMI report (Li et al., 2024b), this study calculates 25 sub-routes within the four major routes, which are shown in Fig. 1's "Total 25 routes of delivery datasets." The optimization objective focuses on efficient sub-route allocation, minimizing the total product of transportation distance and transportation volume while maintaining the maximum supply capacity constraints of hydrogen-producing provinces and ensuring fulfilment of hydrogen-consuming province demands as established in the source projections. This distance-volume optimization determines the most efficient distribution of predetermined total volumes across available sub-routes rather than exploring alternative demand configurations. The optimization approach is constrained by the fixed nature of major route-level supply-demand data from the RMI source (Li et al., 2024b), which limits the scope for comprehensive demand sensitivity analysis. Alternative demand scenarios would require fundamental revision of underlying production capacity and consumption assumptions along with access to detailed regional development projections that extend beyond currently available data sources. The optimization methodology provides efficient allocation solutions within established supply-demand frameworks while acknowledging that future research should incorporate demand pattern sensitivity as more detailed scenario data becomes accessible. Detailed information on these optimized sub-routes is provided in Supplementary Table 2.

The utilization of real-world transportation distances across the 25 optimized sub-routes represents a fundamental methodological advancement beyond conventional sensitivity analysis approaches. Unlike hypothetical distance scenarios, the actual distances derived from China's hydrogen infrastructure projections capture complex interdependencies between spatial patterns, infrastructure constraints, and supply-demand optimization that cannot be replicated through arbitrary distance variations. The heterogeneous spatial distribution of renewable energy resources and hydrogen demand centers creates specific distance clusters ranging from 447 km to 2341 km, reflecting actual supply-demand geography and revealing infrastructure efficiency insights that uniform distance assumptions would obscure.

For the delivery distances of hydrogen along the sub-routes, different estimation methods are used depending on the transportation modes. For trucks and ships, distances along roads and waterways are estimated based on actual map distances. For pipelines and UHV cables, terrain factors are used to estimate distances, as the current pipeline and cable networks are under development. The terrain factor for pipelines is derived from a report by China National Petroleum Corporation (CNPC) (CNPC, 2013), calculated as the ratio of the actual length to the geographical straight-line distance of the three existing West-East Gas Pipelines. Similarly, the terrain factor for UHV cables is based on the ratio of actual length to straight-line distance for China's existing UHV cable projects (International Energy Network (in-en.com), 2020).

This study focuses on the transportation impacts of hydrogen and hydrogen carriers. Therefore, the lifecycle stages related to hydrogen production and the infrastructure or equipment involved in transportation are not included. However, the re-liquefaction process for liquid hydrogen transportation is considered, as it plays a role in maintaining the physical state of liquid hydrogen during shipping. For liquid hydrogen shipping, the energy use and emissions from re-liquefaction are accounted for, as re-liquefaction equipment is typically installed on ships. The data and calculation methods for liquid hydrogen re-liquefaction during shipping are derived from the study by Lee et al. (2022). Potential losses during the delivery stage are incorporated into the model based on carrier-specific characteristics and transport modes. For UHV transmission, an electrical loss rate of 1.5% per 1000 km is applied based on Akira (2020), reflecting transmission losses in ultra-high voltage power lines. For other transport modes, loss rates follow GREET model default parameters: 5% for ship transport (accounting for boil-off losses for cryogenic carriers and handling losses during loading/unloading operations) and 0% for pipeline and truck transport (reflecting the enclosed nature of these systems with minimal leakage under normal operating conditions). Energy consumption for re-compression (pipeline CGH_2) and re-liquefaction (ship-based LH_2) is explicitly modeled to account for processes required to maintain carrier integrity during extended transport distances. *Re*-liquefaction is not considered in the case of liquid hydrogen truck transportation, as such equipment is rarely used on trucks. Goita et al. (2025) found that hydrogen's climate benefits depend on its production pathway, with renewable-powered electrolysis reducing emissions and SMR-based hydrogen having higher impacts. They also found that hydrogen leakage has minimal environmental impacts in terms of emissions but emphasized the need for sector-specific strategies to maximize decarbonization benefits. Therefore, hydrogen leakage impacts will not be considered in this study, but the leakage of carriers such as methanol, which directly emits greenhouse gases, will be included.

While this study uses the GREET model developed by Argonne National Laboratory in the United States and incorporates reaction material inventory data from the European Commission, Joint Research Centre, the inputs including energy structure and other foundational data have been adjusted to reflect the conditions in China and its provinces. This methodological adjustment is reasonable and supported by relevant literature studies (Liu et al., 2025b; Li et al., 2024a).

3.3. Analytical framework for hydrogen supply chain and evaluation criteria

For the calculations and analysis, the GREET model was applied to perform energy consumption and emissions calculations. As discussed in Sections 3.1 and 3.2, the system boundaries exclude hydrogen production and infrastructure equipment, focusing on the energy consumption and emissions during the pre-delivery, delivery, and post-delivery stages. Energy consumption refers to the energy required for the processes themselves, excluding the energy content carried by the carrier (e.g., the inherent calorific value of CGH_2, which is itself a fuel). For emissions, the "GHG-100" parameter from the GREET model was selected, which represents the environmental greenhouse gas impact of a process over a 100-year timeframe.

Based on the framework of the delivery system proposed in this study, the calculation principles and logic for estimating the emissions and other potential impacts (such as energy consumption) of the delivery system are as follows:

$$EI_{delivery\ system} = EI_{pre-delivery} + EI_{delivery} + EI_{post-delivery} \tag{1}$$

$$EI_{phase} = \sum_{i=1}^{n} EI_i \tag{2}$$

In Eq. (1), EI represents the environmental impact, and $EI_{delivery\ system}$ denotes the total environmental impact of the entire delivery system. This total impact is calculated as the sum of the environmental impacts from the three stages: pre-delivery, delivery, and post-delivery.

For each phase, as shown in Eq. (2), the environmental impact EI_{phase} is the summation of the environmental impacts of all processes involved within that phase. For example, in the pre-delivery stage of a carrier such as NH_3 (ammonia), multiple processes including production and liquefaction contribute to the overall impact, rather than a single process.

Beyond using the GREET model for calculations, further data processing was conducted using software such as Python. This included the following steps: converting all GREET calculation results into per-unit emissions or energy consumption values based on 1 kg of hydrogen equivalent, performing weighted average calculations for the 25 routes to derive data for each transportation mode, and disaggregating and combining data for the pre-delivery, delivery, and post-delivery stages. The processed data was then visualized through plotting for presentation of the results. Furthermore, a comparative analysis with existing literature is conducted in the Discussion section to validate the reasonableness of the calculated results across different hydrogen delivery modes.

4. Results and analysis

The analysis reveals four main findings across the 2030–2060 period. First, UHV-electricity consistently achieves the lowest emissions across 88% of sub-routes (22 of 25), decreasing from 0.14–1.44 kg CO_2eq/kg H_2eq in 2030 to 0.03–0.31 kg CO_2eq/kg H_2eq by 2060. Second, regional electricity profiles strongly shape route-level emissions: for the same delivery mode, Pipeline-CGH_2 emits 1.98 kg CO_2eq/kg H_2eq for Inner Mongolia–Shanxi but only 0.64 kg CO_2eq/kg H_2eq for Yunnan–Guizhou in 2030. Third, the penalty for non-optimal mode selection is highly uneven across regions, ranging from only 0.91 versus 0.77 kg CO_2eq/kg H_2eq for Tibet–Fujian in 2030 to 0.47 versus 0.03 kg CO_2eq/kg H_2eq for Inner Mongolia–Shanxi in 2060. Fourth, waterway availability provides only limited and declining benefits, with ship transport remaining competitive in only one of three waterway-accessible sub-routes in 2030 and losing this advantage by 2060. These findings underscore that hydrogen infrastructure planning must be tailored to regional characteristics rather than applying uniform national strategies, with the importance of proper mode selection intensifying over time.

Given the extensive dataset in this study, the results section is structured to provide comprehensive insights into both emission composition and spatial patterns. Section 4.1 decomposes emissions by lifecycle stage (pre-delivery, delivery, and post-delivery) to identify the proportional contributions of each phase across different delivery modes and reveal which stages dominate total emissions. Section 4.2 examines spatial heterogeneity across 25 sub-routes, demonstrating how provincial energy profiles and infrastructure availability create location-specific optimal delivery pathways. Section 4.3 aggregates sub-route emissions to the main route level, presenting heatmaps that visualize temporal emission trends across China's four major hydrogen transport routes from 2030 to 2060. Section 4.4 isolates the relationship between delivery-stage emissions and transport distance, using scatter plots and trend analysis to quantify mode-specific distance sensitivities.

This structure progressively builds understanding from emission mechanisms (Section 4.1) through spatial variations (Section 4.2) to route-level patterns (Section 4.3) and distance relationships (Section 4.4). While Sections 4.1, 4.2, and 4.3 calculate emissions in units of kg CO_2eq/kg H_2eq to indicate the relationship between emissions and delivery volume, Section 4.4 specifically addresses how emissions scale with transport distance. Together, these analyses provide the foundation for understanding how mode selection, regional characteristics, and infrastructure decisions interact to shape hydrogen delivery emissions across China.

4.1. Lifecycle stage decomposition of hydrogen delivery emissions

Section 4.1 decomposes hydrogen delivery emissions by lifecycle stage to reveal the proportional contributions of pre-delivery, delivery, and post-delivery phases across different modes and spatial contexts.

Fig. 2 is divided into two subfigures, Fig. 2 (a) and Fig. 2 (b), to account for differences in the calculation and comparison basis across hydrogen delivery modes. Fig. 2 (a) includes eight delivery modes, with calculations based on a weighted average from all four routes, enabling mode comparison. Fig. 2 (b) focuses on four ship-related modes, with

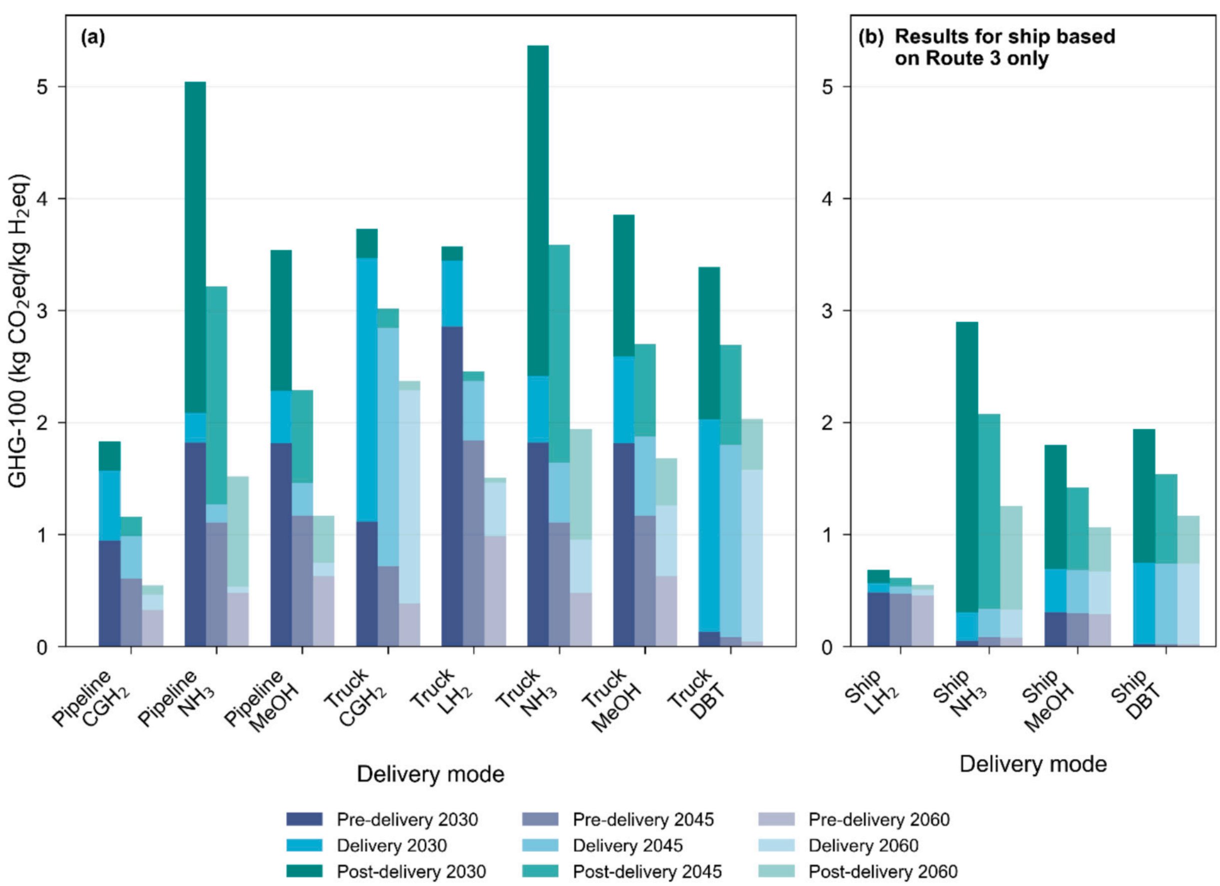

Fig. 2. Lifecycle stage contributions to GHG emissions (kg CO_2eq/kg H_2eq) across hydrogen delivery modes for 2030, 2045, and 2060. (a) Eight delivery modes calculated using turnover-weighted averages across Routes 1–4. (b) Four ship-based modes calculated specifically for Route 3, the only route with suitable inland waterway infrastructure. Abbreviations: CGH_2-compressed gas hydrogen; LH_2-liquid hydrogen; NH_3-ammonia; MeOH-methanol; DBT-dibenzyltoluene.

calculations based on Route 3, which is the only route with suitable inland waterway conditions for ship-based transport. This separation ensures comparisons, as the weighted averages for the modes in Fig. 2 (a) and Fig. 2 (b) are derived from different route scopes.

The purpose of Fig. 2 is to decompose GHG emissions into three lifecycle stages: pre-delivery, delivery, and post-delivery and to observe how the proportions of these stages vary across delivery modes and years (2030, 2045, and 2060). While Fig. 2 shows that UHV-Electricity produces the lowest modeled GHG emissions, its inclusion in Fig. 2 would make its contributions nearly imperceptible. Moreover, under the defined system boundary, emissions for UHV-Electricity arise only from electricity losses during delivery, meaning there are no differences or comparable scenarios across lifecycle stages for this mode. Thus, UHV-Electricity is excluded from Fig. 2, as its inclusion is neither necessary nor aligned with the figure's focus.

Ship-LH_2 shows emissions of 0.68, 0.62, and 0.55 kg CO_2eq/kg H_2eq in 2030, 2045, and 2060 respectively. These relatively low values among ship modes result from two factors: (1) Route 3's waterway infrastructure connects provinces with lower grid emission factors, and (2) despite energy-intensive liquefaction, the cleaner electricity reduces pre-delivery emissions. However, as demonstrated in Section 4.2, this performance is limited to specific geographic contexts and does not generalize across waterway routes.

Ship-based delivery modes show varying emission levels. Ship-LH_2 emissions decreased by 8.82% from 2030 to 2045 and 11.29% from 2045 to 2060. Other ship-based modes including Ship-NH_3, Ship-MeOH, and Ship-DBT also showed declining emissions over time, with Ship-NH_3 recording 2.90 kg CO_2eq/kg H_2eq in 2030, declining by 28.62% to 2045 and 39.13% to 2060. Despite these reductions, ship modes generally maintain higher emissions than pipeline alternatives, particularly when accounting for carrier conversion losses.

Pipeline and truck-based delivery modes show emissions of 5.04 and 5.37 kg CO_2eq/kg H_2eq respectively for Pipeline-NH_3 and Truck-NH_3 in 2030. Carrier-based modes such as those involving NH_3 and MeOH often have high post-delivery emissions due to the energy demands of hydrogen extraction or conversion. For example, in 2030, the post-delivery emissions of Pipeline-NH_3 were about 2.95 kg CO_2eq/kg H_2eq, making a contribution to the total emissions. Pipeline-NH_3 emissions decreased by around 36.31% from 2030 to 2045 and approximately 52.65% from 2045 to 2060. For Truck-NH_3, the decline was about 33.15% from 2030 to 2045 and around 46.07% from 2045 to 2060.

Pre-delivery emissions vary by delivery mode and carrier. In 2030, Truck-LH_2 had pre-delivery emissions of 2.86 kg CO_2eq/kg H_2eq due to hydrogen liquefaction, while Ship-DBT had 0.02 kg CO_2eq/kg H_2eq. Truck-LH_2's pre-delivery emissions decreased by 35.66% from 2030 to 2045 and 46.20% from 2045 to 2060. For truck-based modes, the delivery stage contributes substantially to total emissions. Truck-CGH_2 had delivery emissions of 2.35 kg CO_2eq/kg H_2eq in 2030, accounting for over 60% of total emissions, declining by 9.79% to 2045 and 10.38% to 2060. Post-delivery emissions for Truck-NH_3 decreased by 34.24% from 2030 to 2045 and 48.97% from 2045 to 2060.

Fig. 2 presents lifecycle stage-specific GHG emissions for various hydrogen delivery modes in 2030, 2045, and 2060. All delivery modes show declining total emissions over time, reflecting decarbonization efforts and technological advancements. While total emissions decreased, the relative contributions of the three lifecycle stages remained consistent within each mode across time points. These results indicate the influence of regional energy profiles, carrier selection, and delivery mode on total GHG footprint. While Ship-LH_2 demonstrates lower emissions within Route 3's specific context, the subsequent spatial analysis reveals that ship transport's competitiveness is highly constrained by geographicand infrastructure factors.

4.2. Spatial heterogeneity in hydrogen delivery emissions

The spatial analysis of 25 sub-routes reveals substantial heterogeneity in hydrogen delivery emissions driven by regional energy profiles, infrastructure availability, and geographical constraints. Table 2 presents representative routes demonstrating how spatial factors override distance considerations in determining optimal delivery pathways across three time periods.

The sub-route analysis reveals three distinct spatial patterns that fundamentally shape hydrogen delivery emissions across China.

First, provincial energy profiles emerge as the dominant factor determining mode performance. Routes originating from high-carbon provinces exhibit systematically higher emissions across all delivery modes compared to routes from renewable-rich provinces. For instance, the Inner Mongolia-Shanxi route shows Pipeline-CGH_2 emissions of 1.98 kg CO_2eq/kg H_2eq in 2030, while the Yunnan-Guizhou route achieves only 0.64 kg CO_2eq/kg H_2eq despite comparable pipeline lengths. This difference reflects the contrast between Inner Mongolia's coal-dominated grid at 0.85 kg CO_2/kWh and Yunnan's hydropower-based system at 0.12 kg CO_2/kWh, which causes Pipeline-CGH_2 emissions to differ by a factor of 3.1 between the two routes. The pattern extends to all energy-intensive modes, with routes from Tibet, benefiting from a grid intensity of only 0.08 kg CO_2/kWh, consistently achieving 40–60% lower emissions than routes from fossil-dependent provinces.

Second, infrastructure availability creates discontinuous emission landscapes that cannot be predicted from distance or geographical proximity alone. Among the 25 sub-routes analyzed, only 3 have waterway access—Sichuan-Hubei, Hubei-Jiangsu, and Hubei-Hunan. Notably, ship transport demonstrates competitive performance only in the Sichuan-Hubei route, achieving 0.14 kg CO_2eq/kg H_2eq with Ship-DBT in 2030, comparable to UHV-Electricity's 0.15 kg CO_2eq/kg H_2eq. However, by 2060, this advantage reverses as grid decarbonization benefits UHV more than ship transport, with emissions declining to 0.04 versus 0.12 kg CO_2eq/kg H_2eq respectively. For the Hubei-Jiangsu and Hubei-Hunan routes, ship-based delivery consistently shows higher emissions than UHV alternatives across all time periods. The limited benefit occurs because conversion losses for chemical carriers, with NH_3 achieving only 85% round-trip efficiency and MeOH only 65%, largely offset the advantages of waterway transport.

Third, the emission penalty of choosing a non-optimal mode varies sharply across regional contexts and becomes more pronounced over time. In high-carbon routes, the gap between the best-performing and alternative modes is large and widens further as the grid decarbonizes. For Inner Mongolia–Shanxi, Pipeline-CGH_2 emits 1.98 kg CO_2eq/kg H_2eq in 2030 compared with 0.14 kg CO_2eq/kg H_2eq for UHV-Electricity, and 0.47 kg CO_2eq/kg H_2eq in 2060 compared with only 0.03 kg CO_2eq/kg H_2eq. By contrast, routes from cleaner source regions show much smaller penalties. For Tibet–Fujian, Pipeline-MeOH emits 0.91 kg CO_2eq/kg H_2eq in 2030 versus 0.77 kg CO_2eq/kg H_2eq for UHV-Electricity, and 0.23 versus 0.21 kg CO_2eq/kg H_2eq in 2060. These results indicate that infrastructure investments in high-carbon regions can deliver much larger emission reductions, whereas the additional gains from mode optimization are smaller in already low-carbon regions. Expressed as ratios, the non-optimal option produces emissions only about 1.1 times those of the optimal mode for Tibet–Fujian by 2060, but about 15.7 times for Inner Mongolia–Shanxi.

4.3. Main route-level GHG emissions from hydrogen delivery systems

To explore the spatial and temporal dynamics of hydrogen delivery systems, Section 4.3 focuses on route-level GHG emissions, presenting an analysis of lifecycle emissions across China's four transport routes.

Fig. 3 presents a comprehensive analysis of lifecycle GHG emissions from hydrogen delivery systems across China's four main transport routes. The figure displays heatmaps (a-d) showing emission intensities for each route, with detailed geographic and capacity information. Route 1 connects Inner Mongolia to northeastern and northern China (Heilongjiang, Jilin, Liaoning, Beijing-Tianjin-Hebei, Shanxi) with a 2060 capacity of 5.44 Mt./year. Route 2 links China's northwest

Table 2
Spatial heterogeneity in hydrogen delivery emissions across representative routes.

Route	Optimal Mode	Emissions (kg CO_2eq/kg H_2eq)			Alternative Mode	Emissions (kg CO_2eq/kg H_2eq)		
		2030	2045	2060		2030	2045	2060
High-carbon source regions								
Inner Mongolia→Shanxi	UHV-Electricity	0.14	0.07	0.03	Pipeline-CGH_2	1.98	0.87	0.47
Xinjiang→Guangdong	UHV-Electricity	1.44	0.60	0.31	Truck-DBT	3.21	2.98	2.81
Gansu→Henan	UHV-Electricity	0.49	0.22	0.11	Pipeline-CGH_2	1.52	0.55	0.24
Low-carbon source regions								
Yunnan→Guizhou	UHV-Electricity	0.19	0.13	0.06	Pipeline-CGH_2	0.64	0.41	0.17
Tibet→Chongqing	UHV-Electricity	0.45	0.30	0.14	Pipeline-MeOH	0.88	0.52	0.21
Tibet→Fujian	UHV-Electricity	0.77	0.45	0.21	Pipeline-MeOH	0.91	0.54	0.23
Waterway-accessible routes								
Sichuan→Hubei	Ship-DBT	0.14	0.13	0.12	UHV-Electricity	0.15	0.08	0.04

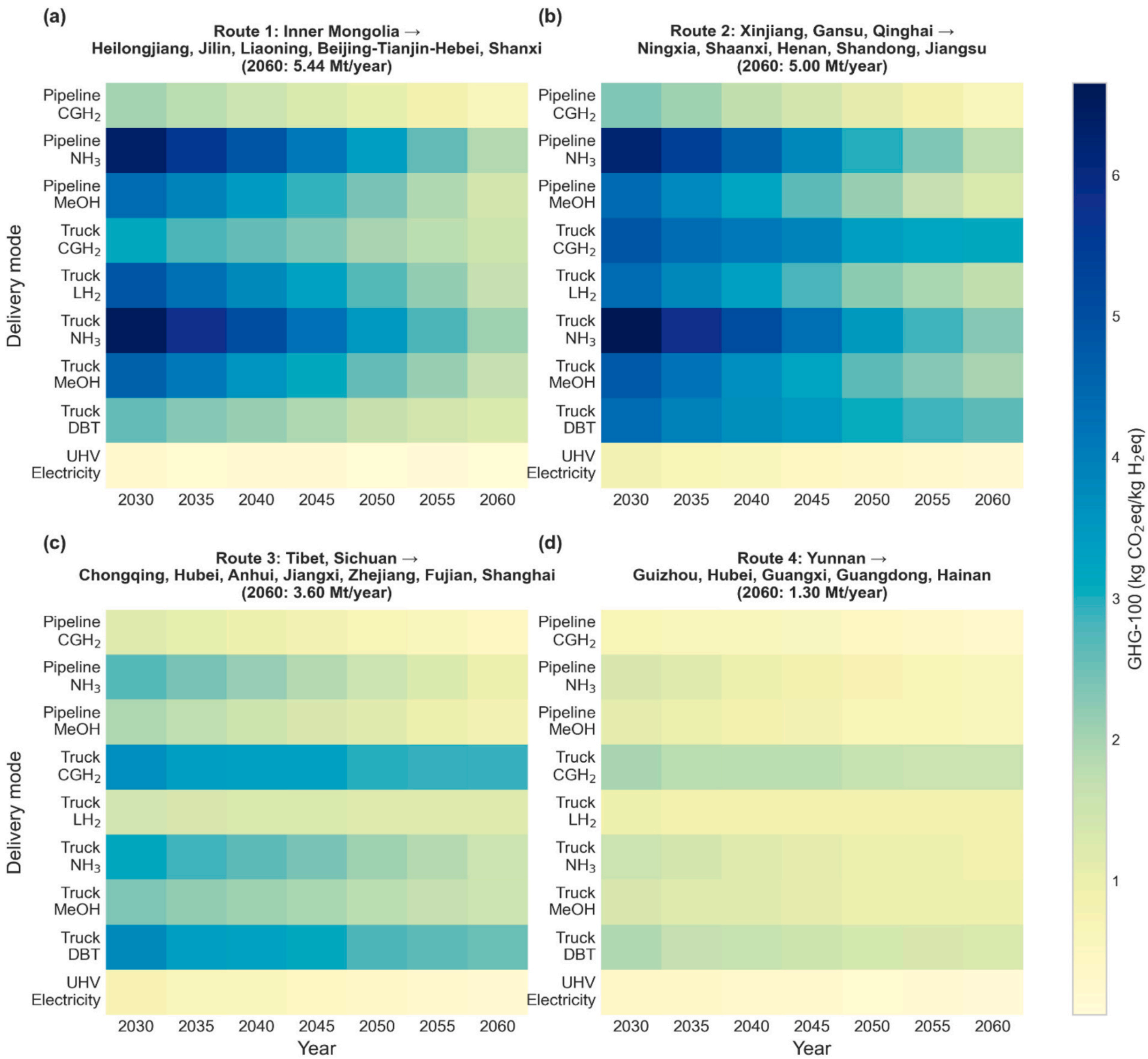

Fig. 3. Lifecycle GHG emissions of hydrogen delivery modes across China's major routes (2030–2060). Heatmaps show emission intensities (kg CO_2eq/kg H_2eq) calculated using delivery amount-weighted averages. Subplot titles indicate route geography and 2060 capacity. Abbreviations: CGH_2-compressed gas hydrogen; LH_2-liquid hydrogen; NH_3-ammonia; MeOH-methanol; DBT-dibenzyltoluene; UHV-ultra high voltage.

(Xinjiang, Gansu, Qinghai) to central and eastern regions (Ningxia, Shaanxi, Henan, Shandong, Jiangsu) with 5.00 Mt./year capacity. Route 3 spans from Tibet and Sichuan to eastern coastal areas (Chongqing, Hubei, Anhui, Jiangxi, Zhejiang, Fujian, Shanghai) with 3.60 Mt./year capacity. Route 4 connects Yunnan to southern China (Guizhou, Hubei, Guangxi, Guangdong, Hainan) with 1.30 Mt./year capacity.

The heatmaps visualize GHG emissions (kg CO_2eq/kg H_2eq) across nine delivery modes (vertical axis) and seven time periods from 2030 to 2060 (horizontal axis), encompassing all three delivery phases: pre-delivery, delivery, and post-delivery. All emission values are calculated using delivery amount-weighted averages of constituent sub-routes within each route, thus representing route-level performance. The color intensity corresponds to emission levels, with darker shades indicating higher emissions.

The analysis of lifecycle GHG emissions across China's hydrogen transport routes reveals distinct spatiotemporal patterns and modal differences. All delivery modes demonstrate declining trends from 2030 to 2060, with UHV-Electricity showing approximately 78–79% reduction across all routes, corresponding to its reliance on the national grid's average emission factor. Pipeline-CGH_2 shows more varied improvement rates ranging from 58% to 73% across routes, indicating heterogeneous emission reduction trajectories for different transport infrastructures.

Geographic disparities emerge prominently across the four routes. Route 4 consistently exhibits the lowest emission intensities despite having the smallest transport capacity of 1.30 Mt./year, with Pipeline-CGH_2 emissions approximately one-third of those in Routes 1 and 2 in 2030. This pattern extends to truck transport modes, where Route 4 shows substantially lower emissions compared to other routes. Route 2 displays the highest emissions for most truck-based modes, maintaining elevated levels even by 2060, particularly for compressed gas and DBT carriers.

A clear modal hierarchy emerges across all routes. UHV-Electricity consistently demonstrates the lowest emissions, achieving 0.050–0.170 kg CO_2eq/kg H_2eq by 2060. Pipeline-CGH_2 ranks second with emissions below 0.65 kg CO_2eq/kg H_2eq by 2060. Among truck-based transport modes, DBT shows relatively favorable performance while NH_3 delivery typically exhibits the highest emissions. Notably, Route 3's truck transport demonstrates limited improvement over the study period, with Truck-LH_2 declining only 14% and Truck-CGH_2 decreasing by 20%, contrasting sharply with the 50–65% reductions observed for the same modes in Route 1.

The rate of emission reduction varies significantly across transport modes and routes. While some truck modes achieve reductions exceeding 60% in certain routes, others show minimal improvement of less than 20% over the 30-year period. Route 2's Truck-CGH_2 exhibits a unique pattern with only 36% reduction despite the extended timeframe. The lifecycle stage analysis reveals that truck transport emissions are dominated by the delivery stage that relies on fossil fuel combustion, explaining the limited emission reductions as delivery-stage emissions remain largely unaffected by electricity grid improvements that primarily benefit pre- and post-delivery stages.

These results demonstrate substantial variation in emission trajectories based on delivery mode and route characteristics. The consistent low emissions of UHV-Electricity and Pipeline-CGH_2 across routes indicate the advantages of infrastructure-based modes. The persistence of high emissions in truck-based transport, particularly for routes with limited improvement rates, combined with Route 4's emissions being 50–70% lower than other routes for several modes, highlights the importance of mode selection and route-specific considerations in hydrogen transport planning. The differential improvement patterns suggest that uniform hydrogen transport strategies would be insufficient given the diverse emission profiles observed across China's transport routes.

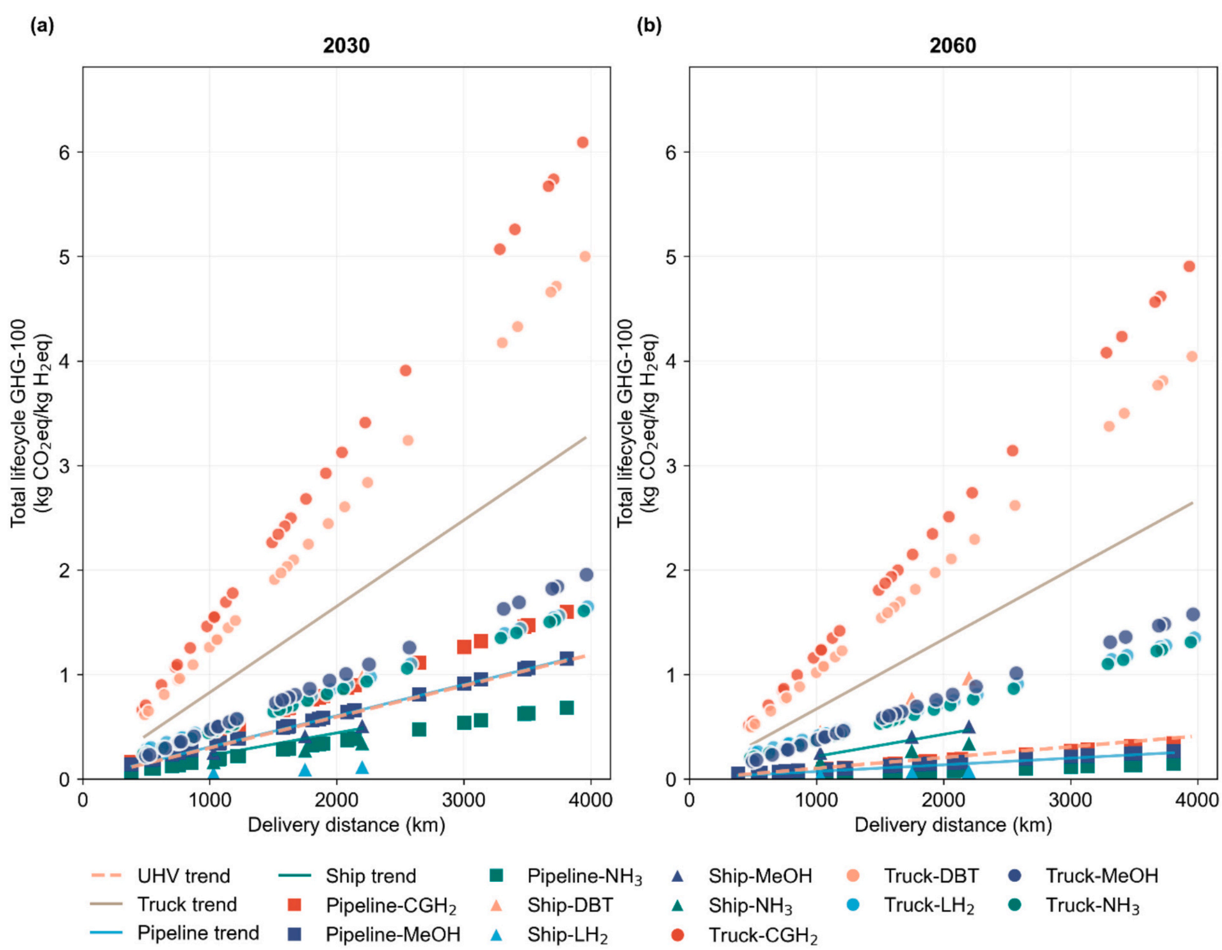

Fig. 4. Distance impact on delivery stage emissions: 2030 vs. 2060.

4.4. Variation of delivery-stage emission intensity with transport distance

Section 4.4 examines how delivery-stage emissions vary with transport distance, using scatter plots and trend analysis to analyze mode-specific efficiencies in 2030 and 2060.

Fig. 4 depicts the relationship between emissions at the delivery stage and delivery distance for 2030 and 2060. Scatter points illustrate the emission levels, while trend lines calculated through a weighted averaging process characterize the trends for different delivery tools (Truck, Pipeline, UHV, Ship). When incorporating pre-delivery and post-delivery stages, the total life-cycle emissions from 25 sub-routes showed no discernible trend with delivery distance. This is because transport distance is not an independent variable across supply chain routes; rather, each route is characterized by a unique combination of three interrelated factors: the transport distance, the energy mix of the supply province (affecting hydrogen production and hydrogenation), and the energy mix of the demand province (affecting dehydrogenation). These factors are intrinsically coupled and cannot be isolated, as they are jointly defined by the geographic characteristics of each specific route. Consequently, routes with similar distances may exhibit substantially different total emissions due to variations in provincial energy structures, while routes with vastly different distances may show similar total emissions when energy mix differences offset the distance effect. Thus, the visualization focuses on the delivery stage, where distance serves as the primary determinant of emissions, enabling clearer and more interpretable trend analysis.

From a temporal perspective, the emission levels of all transportation modes have been reduced, with these emission reductions attributed to the optimization of energy structures and the decrease in the carbon intensity of energy structures. When comparing the same transportation distance, from 2030 to 2060, emissions from trucks as a delivery mode decreased by approximately 19%; pipeline transportation achieved a reduction of about 78.60%; the emission reduction of ship transportation is related to the carrier type. In the scenario where liquid hydrogen (LH_2) serves as the carrier, emissions during transportation are reduced by 37.71%, while other carriers show a reduction of approximately 1.00%. This discrepancy arises from the re-liquefaction process in LH_2 shipping, which relies on the energy structure of the year (calculated based on electricity). Therefore, compared to other carriers with stable physical properties, LH_2 demonstrates emission reduction effects in the delivery process over time; ultra-high voltage (UHV) transportation achieves an emission reduction of approximately 65.39%.

Considering distance variations, the emission levels of all transportation modes increase with longer distances. The trend of scatter plots and fitted slopes reflects the rate of emission level changes with distance. Among them, truck-based modes exhibit changes in emission levels with distance, with compressed gaseous hydrogen (CGH_2) and a carrier (DBT) representing the two modes with high emission levels. In 2030, the emission changes in pipeline modes were higher than that of ships, but by 2060, the trend slowed down to be lower than that of ships. One reason is that the emission changes of ship modes are not significant (it is assumed that ships use diesel as fuel, and the emission reduction of diesel production in China over time is not as significant as the emission reduction of the power grid structure). The other reason is that after China proposed the concepts of carbon peaking and carbon neutrality, policy support for electrification and power grid emission reduction has led to emission reduction effects.

This study examines emission impacts across the supply chain lifecycle. For sustainable zero-carbon development, emission reduction in all three supply chain stages is necessary. In the delivery stage, CGH_2 suits short-distance hydrogen delivery without requiring additional conversion reactions, though truck-based CGH_2 emissions increase substantially with distance. For long-distance transportation, pipelines and UHV show lower emission growth rates, while ship availability depends on waterway infrastructure. Supply chain mode selection depends on multiple factors, with emissions representing a key consideration.

5. Discussion

5.1. Comparison with other references

To demonstrate the consistency with prior studies, this study compares findings with similar literature on hydrogen and hydrogen carrier supply chain environmental assessments. Given that scenarios across various hydrogen supply chain environmental studies are not entirely consistent, the logic of comparison is that emissions from the same type of delivery mode (combination of transportation vehicles and carriers) should exhibit overlapping ranges with differences, and any discrepancies should have reasonable explanations.

Based on numerical values extracted from figures in the literature, de Kleijne et al. (2024) reported delivery emissions for Pipeline-CGH_2 ranging from 0.50 to 3.91 kg CO_2eq/kg H_2, which aligns with the research results of 0.45–2.68 kg CO_2eq/kg H_2. For Ship-LH_2, de Kleijne et al. (2024) obtained 1.07–1.67 kg CO_2eq/kg H_2eq, while the research results of 0.55–0.70 kg CO_2eq/kg H_2eq are lower due to cleaner electricity supply in waterway transport source provinces. For Ship-NH_3, de Kleijne et al. (2024) reported 2.1–2.49 kg CO_2eq/kg H_2eq, while the research results of 1.59–3.58 kg CO_2eq/kg H_2eq are within range. However, the study shows higher proportional contributions from pre-delivery stages compared to de Kleijne et al.'s (2024) results. This occurs because de Kleijne et al. (2024) assumed clean renewable electricity (37 g CO_2eq/kWh) for hydrogen compression and liquefaction, while the study used average local grid emission factors, which are higher and make energy-intensive pre-delivery processes contribute more to the overall carbon footprint.

Cho et al. (2024) also conducted environmental impact analysis for the H_0DBT-H_{18}DBT LOHC system. For LOHC ship transport processes, emissions ranged from 0.16 to 0.66 kg CO_2eq/kg H_2 (data extracted from figure in the original literature), corresponding to transport distances within the baseline range of 1700 km to 5000 km. These values are lower compared to this study's average result of 0.72 kg CO_2eq/kg H_2eq. Given that all transport routes discussed in this study do not exceed 3000 km, this discrepancy can be attributed to the fact that Cho et al.'s research focused on international maritime transport, where ocean-going vessels have higher cargo capacities than inland waterway transport, resulting in lower emissions per unit mass when distributed across the larger transport volumes.

The comparative analysis across different delivery modes reveals that emission results for electricity-intensive processes show discrepancies with other studies, due to inconsistencies in the energy mix structures considered in different research contexts.

5.2. Regional heterogeneity and spatially-differentiated infrastructure policy

The sub-route level analysis reveals that spatial heterogeneity in regional energy systems rather than transport distance constitutes the primary determinant of hydrogen delivery emissions. This finding represents a departure from conventional hydrogen logistics studies that emphasize distance-based optimization, and carries significant implications for China's regional hydrogen development strategies.

The disaggregated analysis of 25 sub-routes demonstrates that provincial electricity carbon intensity creates substantial emission variations between routes, even when transport distances are comparable. Routes originating from coal-dominated provinces exhibit systematically higher emissions across all delivery modes compared to routes from hydropower-rich southwestern provinces. This pattern reflects the carbon intensity of electricity consumed during compression, liquefaction, and carrier conversion processes at the source location, which propagates through the entire delivery pathway. Notably, this regional disparity intensifies over time rather than diminishing, as grid decarbonization benefits accrue disproportionately to electricity-dependent transport modes such as UHV transmission. Consequently, the relative advantage of selecting optimal delivery modes in high-carbon regions grows larger approaching 2060, while routes from already-clean provinces maintain stable but moderate differences between modal alternatives.

These spatial patterns suggest a geographically-differentiated approach to hydrogen infrastructure investment across China's major hydrogen routes. For routes connecting northwestern production centers to eastern demand centers, electricity transmission infrastructure warrants priority consideration, as these routes show the largest emission differences between optimal and suboptimal mode selections. The carbon-intensive regional grids in northwestern provinces mean that hydrogen carriers requiring substantial electrical processing particularly compressed gaseous hydrogen and liquefied hydrogen incur disproportionately higher emissions when produced in these regions. In contrast, UHV transmission can leverage planned renewable energy developments in Inner Mongolia and Xinjiang while avoiding the conversion losses associated with chemical carriers.

For routes originating from hydropower-rich southwestern provinces, the emission hierarchy remains consistent with UHV-Electricity as optimal, but the differences between alternative modes are substantially smaller. This indicates greater flexibility in infrastructure deployment, where pipeline systems may complement UHV where terrain complexity or grid capacity constraints exist, without incurring severe environmental consequences. The mountainous geography of these regions often presents engineering challenges for both pipeline construction and transmission line routing, making this flexibility particularly valuable for practical implementation.

The sub-route analysis also reveals that ship-based transport offers limited and geographically-constrained benefits, refining the conclusions drawn from aggregated route-level assessment. While the Sichuan-Chongqing route's favorable waterway performance might suggest broader applicability of inland shipping, disaggregated examination of individual sub-routes indicates that such advantages are highly route-specific. The competitiveness of ship transport depends critically on the carbon intensity of destination province grids where post-delivery processing occurs. Sub-routes terminating in provinces with higher grid carbon intensity show substantially elevated total pathway emissions, eroding any efficiency gains from waterway transport itself. Furthermore, the temporal trajectory of ship-based alternatives diverges unfavorably from grid-connected modes: as provincial grids decarbonize at varying rates, routes that currently show marginal ship advantages may see these benefits reverse within the study timeframe. These findings indicate that inland waterway infrastructure development for hydrogen transport should be approached with caution, with investment decisions contingent on specific route characteristics and temporal projections rather than general assumptions about waterway efficiency.

Based on these spatial heterogeneity patterns, China's hydrogen infrastructure planning should adopt region-specific strategies rather than uniform national approaches. First, priority deployment of electricity transmission capacity should focus on northwestern-to-eastern routes, where the environmental consequences of infrastructure misallocation are most pronounced and where grid-connected alternatives can leverage the region's renewable energy resource endowments. Second, infrastructure development in southwestern routes should accommodate multiple modal options, recognizing that the environmental differences between alternatives are smaller and that geographic constraints may favor hybrid solutions combining transmission and pipeline elements. Third, waterway infrastructure investments should be selective rather than comprehensive, limited to specific high-performing route segments where detailed analysis confirms sustained competitiveness, rather than pursuing broad network expansion based on aggregated assessments. Finally, infrastructure planning frameworks should incorporate temporal adaptation mechanisms that accommodate modal transitions as grid decarbonization progresses, rather than locking in current technology choices for multi-decade investment horizons.

5.3. Mode-specific performance and technological implications

The lifecycle stage decomposition reveals emission profiles that inform technology development priorities. Truck-based transport exhibits delivery-stage dominance, suggesting that improvements in vehicle efficiency and alternative fuel adoption could yield benefits. Conversely, carrier-based modes show post-delivery emissions, indicating that advancing dehydrogenation and conversion technologies should be prioritized for NH_3 and LOHC pathways.

Ship-based transport's performance in Route 3, particularly for LH_2 delivery, demonstrates the importance of leveraging existing waterway infrastructure and regional clean energy advantages. The temporal transition of ship-based NH_3 delivery from disadvantage in 2030 to advantage by 2060 indicates that technological learning and operational optimization can alter mode competitiveness, suggesting that EIA frameworks should account for technology development trajectories rather than current performance alone.

The sub-route analysis refines understanding of ship-based transport performance. While aggregated route-level results initially suggested waterway advantages for certain routes, disaggregated analysis reveals that Ship-LH_2's relatively low emissions of 0.54–0.70 kg CO_2eq/kg H_2eq reflect the specific characteristics of the Sichuan-Hubei route rather than generalizable waterway benefits. The provinces connected by this route benefit from Sichuan's hydropower-dominated grid for pre-delivery processing and Hubei's central logistics position, creating favorable conditions not replicated in other waterway-accessible routes where post-delivery processing in destination provinces with higher grid carbon intensity substantially increases total pathway emissions.

5.4. Distance-emission relationships and system optimization

The distance-emission analysis provides quantitative support for supply chain optimization strategies and infrastructure planning decisions. The emission gradients observed for truck-based CGH_2 transport confirm its suitability for short-distance applications, while the stable performance of pipeline and UHV systems supports their deployment for long-distance hydrogen routes. These findings enable evidence-based infrastructure investment decisions that optimize environmental performance across different transport scenarios.

This finding carries important implications for infrastructure planning: optimizing delivery distance alone yields limited environmental benefits without concurrent attention to regional energy characteristics. For instance, a short-distance route such as Inner Mongolia-Shanxi at 307 km with high-carbon grid produces higher Pipeline-CGH_2 emissions of 1.98 kg CO_2eq/kg H_2eq than a long-distance route such as Tibet-Fujian at 2800 km with clean grid producing 1.86 kg CO_2eq/kg H_2eq. This counterintuitive result emphasizes that spatial optimization must consider energy profiles alongside geographic proximity, and that infrastructure investment decisions based primarily on minimizing transport distance may inadvertently select higher-emission pathways.

The finding that total lifecycle emissions show minimal distance correlation while delivery-stage emissions exhibit strong distance relationships indicates that EIA assessments should differentiate between local distribution impacts and long-distance transmission effects. This insight suggests that regulatory approaches should distinguish between regional hydrogen hubs and intercity transmission infrastructure, with different environmental standards and assessment criteria for each application.

5.5. Limitations and future research directions

Several limitations warrant consideration in interpreting these results. First, the analysis assumes current technological parameters for future projections, potentially underestimating breakthrough innovations in hydrogen technologies. Second, the focus on GHG emissions does not capture other environmental impacts such as air quality, water consumption, or land use changes that may influence policy decisions. Third, economic factors including capital costs, operational expenses, and infrastructure investment requirements are not integrated into the analysis, limiting practical applicability. Fourth, the route optimization is constrained by predetermined supply-demand relationships from the RMI source data, preventing comprehensive sensitivity analysis of alternative demand patterns that may emerge as hydrogen markets develop. Fifth, the loss rates applied across different carriers within the same transport mode are uniform (e.g., 5% for all ship-based carriers), which represents a simplification that does not fully capture carrier-specific behaviors. For instance, LH_2 may experience higher boil-off rates than chemically stable carriers such as DBT or MeOH. Preliminary sensitivity analysis indicates that while absolute emission values are affected by differentiated loss rate assumptions, the relative ranking of pathways and primary conclusions remain unchanged. Nevertheless, future studies with more detailed empirical data on carrier-specific losses could further refine these estimates. Sixth, while leakage rates represent important considerations for hydrogen supply chain assessment particularly regarding transport efficiency, indirect global warming potential effects, and safety implications: the comprehensive evaluation of these multifaceted impacts requires extensive additional analytical frameworks beyond the current study's scope. The complex interactions between leakage phenomena, carrier-specific behaviors, and environmental consequences necessitate dedicated research approaches that would fundamentally expand the present analysis framework.

Future research should incorporate dynamic technology learning curves, multi-criteria environmental assessment, and techno-economic optimization to provide comprehensive decision support. The spatial heterogeneity findings suggest particular value in developing region-specific hydrogen infrastructure roadmaps that integrate provincial energy transition trajectories with transport network planning. Additionally, investigating the sensitivity of results to infrastructure availability and policy scenarios would enhance the robustness of recommendations for hydrogen supply chain development. As hydrogen market projections become more refined and detailed regional scenario data becomes available, demand pattern sensitivity analysis should be integrated to support adaptive infrastructure planning under uncertainty. Comprehensive leakage assessment frameworks should be developed to address the complex interdependencies between hydrogen carrier properties, transport conditions, and environmental impacts.

6. Conclusion

This study presents a spatially-explicit lifecycle assessment of hydrogen delivery systems across four transport routes in China, analyzing 25 sub-routes with 12 delivery modes from 2030 to 2060. The disaggregated sub-route analysis reveals that spatial heterogeneity in provincial energy systems rather than transport distance constitutes the primary determinant of hydrogen delivery emissions. Provincial electricity carbon intensity strongly affects route-level emissions even for the same delivery mode. For example, Pipeline-CGH_2 emissions in 2030 range from 0.64 kg CO_2eq/kg H_2eq for Yunnan–Guizhou to 1.98 kg CO_2eq/kg H_2eq for Inner Mongolia–Shanxi, despite comparable pipeline lengths. The emission penalty of selecting a non-optimal delivery mode is also highly uneven, ranging from 0.91 versus 0.77 kg CO_2eq/kg H_2eq for Tibet–Fujian in 2030 to 0.47 versus 0.03 kg CO_2eq/kg H_2eq for Inner Mongolia–Shanxi in 2060. These results show that infrastructure decisions should be guided not only by distance or connectivity, but also by the carbon intensity of regional energy systems. UHV-Electricity emerges as environmentally optimal across 88% of sub-routes, while ship-based transport demonstrates competitive performance only in the Sichuan-Hubei route, with advantages reversing by 2060.

These findings support regionally-differentiated infrastructure strategies for China's hydrogen economy. Priority deployment of UHV transmission should focus on northwestern-to-eastern routes connecting Inner Mongolia and Xinjiang to demand centers, where environmental consequences of infrastructure misallocation are most severe. Southwestern routes from Tibet, Sichuan, and Yunnan should accommodate flexible multi-modal solutions given smaller emission differences between alternatives. Waterway infrastructure investments should be selective rather than comprehensive, limited to specific route segments where analysis confirms sustained competitiveness.

The spatially-explicit framework developed through this analysis demonstrates that regional energy profiles fundamentally shape delivery system performance, providing methodological approaches applicable to hydrogen infrastructure planning in comparable national contexts. Future research should integrate dynamic technology learning curves, multi-criteria environmental assessment, and techno-economic optimization to support adaptive infrastructure planning as hydrogen markets develop.

Declaration of competing interest

The authors declare that they have no known competing financial interests or personal relationships that could have appeared to influence the work reported in this paper.

Appendix A. Supplementary data

Supplementary data to this article can be found online at https://doi.org/10.1016/j.eiar.2026.108435.

Data availability

Data will be made available on request.

References

Ahn, B., Sohn, H., Liu, J.J., Won, W., 2024. A system-level analysis for long-distance hydrogen transport using liquid organic hydrogen carriers (LOHCs): a case study in Australia–Korea. ACS Sustain. Chem. Eng. 12, 8630–8641. https://doi.org/10.1021/acssuschemeng.4c00330.

Akira, T., 2020. Smart Grid, A Game Changer [WWW Document]. URL. https://www.integralnewenergy.com/?p=30321 (accessed 6.3.25).

Alaba, F.A., Sani, U., Dada, E.G., Mohammed, B.H., 2024. AIoT-enabled smart grids: advancing energy efficiency and renewable energy integration. In: Misra, S., Siakas, K., Lampropoulos, G. (Eds.), Artificial Intelligence of Things for Achieving Sustainable Development Goals. Springer Nature Switzerland, Cham, pp. 59–79. https://doi.org/10.1007/978-3-031-53433-1_4.

Alkhaledi, A.N., Sampath, S., Pilidis, P., 2022. A hydrogen fuelled LH2 tanker ship design. Ships Offshore Struct. 17 (7), 1555–1564. https://doi.org/10.1080/17445302.2021.1935626.

Argonne National Laboratory. GREET® (Greenhouse gases, Regulated Emissions, and Energy use in Technologies) model. https://greet.es.anl.gov/.

Arrigoni, A., Dolci, F., Ortiz Cebolla, R., Weidner, E., D'Agostini, T., Eynard, U., Santucci, V., Mathieux, F., 2024. Environmental Life Cycle Assessment (LCA) Comparison of Hydrogen Delivery Options within Europe. European Commission, Joint Research Centre, Luxembourg.

Balaji, R.K., You, F., 2024. Sailing towards sustainability: offshore wind's green hydrogen potential for decarbonization in coastal USA. Energy Environ. Sci. https://doi.org/10.1039/D4EE01460J.

Baz, A., Logeshwaran, J., Natarajan, Y., Patel, S.K., 2024. Deep fuzzy nets approach for energy efficiency optimization in smart grids. Appl. Soft Comput. 161, 111724. https://doi.org/10.1016/j.asoc.2024.111724.

BloombergNEF, 2020. Hydrogen Economy Outlook. BloombergNEF.

Boretti, A., 2025. Pathways to net zero: scaling renewable energy and hydrogen storage in New Zealand. J. Braz. Soc. Mech. Sci. Eng. 47, 71. https://doi.org/10.1007/s40430-025-05398-z.

Boretti, A., Pollet, B.G., 2024. Hydrogen economy: paving the path to a sustainable, low-carbon future. Int. J. Hydrog. Energy 93, 307–319. https://doi.org/10.1016/j.ijhydene.2024.10.350.

Chen, L., Wang, Y., Jiang, Y., Zhang, C., Liao, Q., Li, J., Wu, J., Gao, X., 2024. Life cycle assessment of liquid hydrogen fuel for vehicles with different production routes in China. Energy 299, 131472. https://doi.org/10.1016/j.energy.2024.131472.

China Daily, 2025. Ordos advances hydrogen innovation for technological breakthroughs [WWW Document]. URL. https://regional.chinadaily.com.cn/ordosen/en/2025-02/14/c_1070417.htm (accessed 3.4.25).

China Electricity Council, 2022. China Electric Power Statistical Yearbook 2021 [WWW Document]. URL. http://www.stats.gov.cn/zs/tjwh/tjkw/tjzl/202302/t20230215_1907998.html (accessed 10.31.23).

China Hydrogen Alliance, 2019. China's Hydrogen Energy and Fuel Cell Industry White Paper. China Hydrogen Alliance.

Cho, H.H., Strezov, V., Evans, T.J., 2024. Life cycle assessment of renewable hydrogen transport by liquid organic hydrogen carriers. J. Clean. Prod. 469, 143130. https://doi.org/10.1016/j.jclepro.2024.143130.

CNPC, 2013. Smart Grid, A Game Changer. CNPC.

de Kleijne, K., Huijbregts, M.A.J., Knobloch, F., van Zelm, R., Hilbers, J.P., de Coninck, H., Hanssen, S.V., 2024. Worldwide greenhouse gas emissions of green hydrogen production and transport. Nat. Energy 9, 1139–1152. https://doi.org/10.1038/s41560-024-01563-1.

Deng, X., Teng, F., Zhang, X., Fan, J.-L., Forsell, N., Reiner, D.M., 2025. Co-deploying biochar and bioenergy with carbon capture and storage improves cost-effectiveness and sustainability of China's carbon neutrality. One Earth 8. https://doi.org/10.1016/j.oneear.2024.12.008.

Drube, T.K., Gerlach, J.M., Leach, T.S., Vogel, B., Klebanoff, L.E., 2024. Exploring variations in the weight, size and shape of liquid hydrogen tanks for zero-emission fuel-cell vessels. Int. J. Hydrog. Energy 80, 1441–1465. https://doi.org/10.1016/j.ijhydene.2024.06.420.

EIT, 2025. City of Hamburg plans to reduce heat energy consumption in public buildings by up to 30 percent this winter [WWW Document]. URL. https://www.eit.europa.eu/news-events/news/city-hamburg-plans-reduce-heat-energy-consumption-public-buildings-30-percent (accessed 3.4.25).

El Hassani, S., Lebrouhi, B.E., Kousksou, T., 2024. A feasibility study of green hydrogen and E-fuels production from a renewable energy hybrid system in the city of Dakhla, Morocco. Int. J. Hydrog. Energy 73, 316–330. https://doi.org/10.1016/j.ijhydene.2024.05.472.

ETC, 2021. Making the Hydrogen Economy Possible: Accelerating Clean Hydrogen in an Electrified Economy. Energy Transitions Commission. URL. https://www.energy-transitions.org/publications/making-clean-hydrogen-possible/ (accessed 8.17.25).

Gambini, M., Guarnaccia, F., Manno, M., Vellini, M., 2024. Feasibility study of LOHC-SOFC systems under dynamic behavior for cargo ships compared to ammonia alternatives. Int. J. Hydrog. Energy 81, 81–92. https://doi.org/10.1016/j.ijhydene.2024.07.224.

Gillette, J.L., Kolpa, R.L., 2008. Overview of Interstate Hydrogen Pipeline Systems. (No. ANL/EVS/TM/08-2). Argonne National Lab. (ANL), Argonne, IL (United States). https://doi.org/10.2172/924391.

Godinho, J., Hoefnagels, R., Braz, C.G., Sousa, A.M., Granjo, J.F.O., 2023. An economic and greenhouse gas footprint assessment of international maritime transportation of hydrogen using liquid organic hydrogen carriers. Energy 278, 127673. https://doi.org/10.1016/j.energy.2023.127673.

Godinho, J., Gomes, J.G., Jiang, J., Sousa, A., Gomes, A., Santos, B.H., Matos, H.A., Granjo, J., Frade, P., Wang, S., Zhang, X., Li, X., Lin, Y., 2024. Supply chains of green hydrogen based on liquid organic carriers inside China: Economic assessment and greenhouse gases footprint. In: Vahidinasab, V., Mohammadi-Ivatloo, B., Shiun Lim, J. (Eds.), Green Hydrogen in Power Systems. Springer International Publishing, Cham, pp. 245–300. https://doi.org/10.1007/978-3-031-52429-5_11.

Goita, E.G., Beagle, E.A., Nasta, A.N., Wissmiller, D.L., Ravikumar, A., Webber, M.E., 2025. Effect of hydrogen leakage on the life cycle climate impacts of hydrogen supply chains. Commun. Earth Environ. 6, 1–10. https://doi.org/10.1038/s43247-025-02141-3.

Gonçalves Dias Ponzi, G., Jacks Mendes dos Santos, V.H., de Medeiros Engelmann, P., Dalla Vecchia, F., 2024. The hydrogen life cycle assessment methodology: an overlooked puzzle piece in harmonizing hydrogen certification and trade. Clean Techn. Environ. Policy 26, 2573–2596. https://doi.org/10.1007/s10098-024-02752-y.

INTEGRAL, 2021. What is next for China's hydrogen supply chain (2) — Storage and Transport [WWW Document]. URL. https://www.integralnewenergy.com/?p=31362.

International Energy Network (in-en.com), 2020. Overview of Domestic Direct Current Transmission Projects in China [WWW Document]. URL. https://power.in-en.com/html/power-2353233.shtml.

ISO, 2006a. ISO 14040:2006 [WWW Document]. ISO. URL. https://www.iso.org/standard/37456.html (accessed 8.19.25).

ISO, 2006b. ISO 14044:2006 [WWW Document]. ISO. URL. https://www.iso.org/standard/38498.html (accessed 8.19.25).

ISO, 2025. Hydrogen Fuel Quality — Product Specification.

Khatiwada, D., Vasudevan, R.A., Santos, B.H., 2022. Decarbonization of natural gas systems in the EU – costs, barriers, and constraints of hydrogen production with a case study in Portugal. Renew. Sust. Energ. Rev. 168, 112775. https://doi.org/10.1016/j.rser.2022.112775.

Kim, S., Park, J., Heo, S., Lee, J.H., 2024. Green hydrogen vs green ammonia: a hierarchical optimization-based integrated temporal approach for comparative techno-economic analysis of international supply chains. J. Clean. Prod. 465, 142750. https://doi.org/10.1016/j.jclepro.2024.142750.

Lee, J., Choi, Y., Che, S., Choi, M., Chang, D., 2022. Integrated design evaluation of propulsion, electric power, and re-liquefaction system for large-scale liquefied hydrogen tanker. Int. J. Hydrog. Energy 47, 4120–4135. https://doi.org/10.1016/j.ijhydene.2021.11.004.

Li, T., Tan, G., Wang, Z., Zhang, B., 2024a. Long Term Outlook on Hydrogen Storage and Transportation Landscape and Technology Evolution in China. Rocky Mountain Institute.

Li, H., Zhang, X., Zhang, C., Ding, Z., Jin, X., 2024b. Application and analysis of liquid organic hydrogen carrier (LOHC) technology in practical projects. Energies 17, 1940. https://doi.org/10.3390/en17081940.

Liu, F., Shafique, M., Luo, X., 2024. Quantifying delayed climate mitigation benefits in electric and fuel cell vehicle deployment for sustainable mobility. Sustainable Prod. Consumption. https://doi.org/10.1016/j.spc.2024.06.001.

Liu, F., Shafique, M., Luo, X., 2025a. Next leap in the sustainable transport revolution: identifying gaps and proposing solutions for hydrogen mobility. Commun. Transp. Res. 5, 100180. https://doi.org/10.1016/j.commtr.2025.100180.

Liu, F., Shafique, M., Luo, X., 2025b. Dynamic lifecycle emissions of electric and hydrogen fuel cell vehicles in a multi-regional perspective. Environ. Impact Assess. Rev. 111, 107695. https://doi.org/10.1016/j.eiar.2024.107695.

Makepeace, R.W., Tabandeh, A., Hossain, M.J., Asaduz-Zaman, Md., 2024. Techno-economic analysis of green hydrogen export. Int. J. Hydrog. Energy 56, 1183–1192. https://doi.org/10.1016/j.ijhydene.2023.12.212.

Masson-Delmotte, V., Zhai, P., Pirani, A., Connors, S.L., Péan, C., Berger, S., Caud, N., Chen, Y., Goldfarb, L., Gomis, M.I., Huang, M., Leitzell, K., Lonnoy, E., Matthews, J.B.R., Maycock, T.K., Waterfield, T., Yelekçi, Ö., Yu, R., Zhou, B. (Eds.), 2021. Climate Change 2021: The Physical Science Basis. Contribution of Working Group I to the Sixth Assessment Report of the Intergovernmental Panel on Climate Change. Cambridge University Press, Cambridge, United Kingdom and New York, NY, USA. https://doi.org/10.1017/9781009157896.

Mittal, S., 2025. California Wildfires: Economic Losses Reach $57bn [WWW Document]. https://www.edie.net/. URL. https://www.edie.net/california-faces-57bn-in-losses-from-catastrophic-wildfires/ (accessed 3.4.25).

Nanninga, N.E., Levy, Y.S., Drexler, E.S., Condon, R.T., Stevenson, A.E., Slifka, A.J., 2012. Comparison of hydrogen embrittlement in three pipeline steels in high pressure gaseous hydrogen environments. Corros. Sci. 59, 1–9. https://doi.org/10.1016/j.corsci.2012.01.028.

Niermann, M., Timmerberg, S., Drünert, S., Kaltschmitt, M., 2021. Liquid organic hydrogen carriers and alternatives for international transport of renewable hydrogen. Renew. Sust. Energ. Rev. 135, 110171. https://doi.org/10.1016/j.rser.2020.110171.

Noh, H., Kang, K., Seo, Y., 2023. Environmental and energy efficiency assessments of offshore hydrogen supply chains utilizing compressed gaseous hydrogen, liquefied hydrogen, liquid organic hydrogen carriers and ammonia. Int. J. Hydrog. Energy 48, 7515–7532. https://doi.org/10.1016/j.ijhydene.2022.11.085.

Qin, B., Wang, H., Liao, Y., Li, H., Ding, T., Wang, Z., Li, F., Liu, D., 2024. Challenges and opportunities for long-distance renewable energy transmission in China. Sustain. Energy Techn. and Assess. 69, 103925. https://doi.org/10.1016/j.seta.2024.103925.

Reddi, K., Elgowainy, A., Rustagi, N., Gupta, E., 2018. Techno-economic analysis of conventional and advanced high-pressure tube trailer configurations for compressed hydrogen gas transportation and refueling. Int. J. Hydrog. Energy 43, 4428–4438. https://doi.org/10.1016/j.ijhydene.2018.01.049.

Ren, Y., Sun, X., Wolfram, P., Zhao, S., Tang, X., Kang, Y., Zhao, D., Zheng, X., 2023. Hidden delays of climate mitigation benefits in the race for electric vehicle deployment. Nat. Commun. 14, 3164. https://doi.org/10.1038/s41467-023-38182-5.

Rey, I., Barrio, V.L., Agirre, I., 2024. Environmental assessment of a hydrogen supply chain using LOHC system with novel low-PGM catalysts: a life cycle approach. Int. J. Hydrog. Energy. https://doi.org/10.1016/j.ijhydene.2024.11.197.

Rumsa, M., John, M., Biswas, W., 2025. Global steel decarbonisation roadmaps: near-zero by 2050. Environ. Impact Assess. Rev. 112, 107807. https://doi.org/10.1016/j.eiar.2025.107807.

Sage, V., Patel, J., Hazewinkel, P., Yasin, Q.U.A., Wang, F., Yang, Y., Kozielski, K., Li, C., 2024. Recent progress and techno-economic analysis of liquid organic hydrogen carriers for Australian renewable energy export – a critical review. Int. J. Hydrog. Energy 56, 1419–1434. https://doi.org/10.1016/j.ijhydene.2023.12.269.

Savickas, R., 2022. Identifying the Differences in between Green, Low-carbon and Renewable Hydrogen. UNEP.

Sayer, M., Ajanovic, A., Haas, R., 2024. Economic and environmental assessment of different hydrogen production and transportation modes. Int. J. Hydrog. Energy 65, 626–638. https://doi.org/10.1016/j.ijhydene.2024.04.073.

Shafique, M., Azam, A., Rafiq, M., Luo, X., 2022. Life cycle assessment of electric vehicles and internal combustion engine vehicles: A case study of Hong Kong. Res. Trans. Econ. 91, 101112. https://doi.org/10.1016/j.retrec.2021.101112.

Shao, T., Peng, T., Zhu, L., Lu, Y., Wang, L., Pan, X., 2024. China's transportation decarbonization in the context of carbon neutrality: a segment-mode analysis using integrated modelling. Environ. Impact Assess. Rev. 105, 107392. https://doi.org/10.1016/j.eiar.2023.107392.

Shen, H., Crespo del Granado, P., Jorge, R.S., Löffler, K., 2024. Environmental and climate impacts of a large-scale deployment of green hydrogen in Europe. Energy Clim. Change 5, 100133. https://doi.org/10.1016/j.egycc.2024.100133.

Sinyoung, S., Jeeraro, A., Udomkun, P., Kunchariyakun, K., Graham, M., Kaewlom, P., 2025. Enhancing CO2 sequestration through corn stalk biochar-enhanced mortar: a synergistic approach with algal growth for carbon capture applications. Sustainability 17, 342. https://doi.org/10.3390/su17010342.

Sun, H., Wang, Z., Meng, Q., White, S., 2025. Advancements in hydrogen storage technologies: enhancing efficiency, safety, and economic viability for sustainable energy transition. Int. J. Hydrog. Energy 105, 10–22. https://doi.org/10.1016/j.ijhydene.2025.01.176.

UNEP, 2009. Guidelines for Social Life Cycle Assessment of Products | UNEP - UN Environment Programme [WWW Document]. URL. https://www.unep.org/resources/report/guidelines-social-life-cycle-assessment-products (accessed 8.19.25).

Wang, B., Liu, G., Zhou, S., Tang, Z., Liu, Z., Deng, N., Wang, Z., 2025a. Can China's renewable energy policy synergies help clean energy transition? Environ. Impact Assess. Rev. 113, 107878. https://doi.org/10.1016/j.eiar.2025.107878.

Wang, T., Su, X., Mei, Y., Xiong, W., 2025b. Climate change intensifies low-carbon transition pressure in China's power system. Environ. Impact Assess. Rev. 114, 107949. https://doi.org/10.1016/j.eiar.2025.107949.

Winnefeld, C., Kadyk, T., Bensmann, B., Krewer, U., Hanke-Rauschenbach, R., 2018. Modelling and designing cryogenic hydrogen tanks for future aircraft applications. Energies 11, 105. https://doi.org/10.3390/en11010105.

Xu, Z., Zhao, N., Yan, Y., Zhang, Y., Zhang, T., Wu, D., Hillmansen, S., Gao, S., 2024. Hydrogen supply chain for future hydrogen-fuelled railway in the UK: transport sector focused. Int. J. Hydrog. Energy 86, 1–13. https://doi.org/10.1016/j.ijhydene.2024.08.397.

Yang, J., Lai, X., Wen, F., Dong, Z.Y., 2024. Green hydrogen credit subsidized renewable energy-hydrogen business models for achieving the carbon neutral future. Int. J. Hydrog. Energy 60, 189–193. https://doi.org/10.1016/j.ijhydene.2024.02.152.

Yin, J., Jia, H., Chen, L., Liu, D., Mei, S., Wang, S., 2024. Optimal scheduling of zero-carbon park considering variational characteristics of hydrogen energy storage systems. Glob. Energy Interconnect. 7, 603–615. https://doi.org/10.1016/j.gloei.2024.10.007.

Yu, Q., Hao, Y., Ali, K., Hua, Q., Sun, L., 2024. Techno-economic analysis of hydrogen pipeline network in China based on levelized cost of transportation. Energy Convers. Manag. 301, 118025. https://doi.org/10.1016/j.enconman.2023.118025.

Zhang, W., Li, Y., Li, H., Liu, S., Zhang, J., Kong, Y., 2024. Systematic review of life cycle assessments on carbon emissions in the transportation system. Environ. Impact Assess. Rev. 109, 107618. https://doi.org/10.1016/j.eiar.2024.107618.

Zhao, Y., 2025. China Records Warmest Temperature in 2024 [WWW Document]. URL. https://www.chinadaily.com.cn/a/202501/02/WS67760c6fa310f1265a1d896b.html (accessed 3.4.25).